Corrugated nanofiber tissue-engineered vascular graft to prevent kinking for arteriovenous shunts in an ovine model

Hiroshi Matsushita, MD,[a] Takahiro Inoue, MD, PhD,[a] Sara Abdollahi, PhD,[a] Enoch Yeung, MBBS,[a] Chin Siang Ong, MBBS, PhD,[a] Cecillia Lui, MD,[a] Isaree Pitaktong,[a] Kevin Nelson, PhD,[b] Jed Johnson, PhD,[b] *and* Narutoshi Hibino, MD, PhD,[a] *Baltimore, Md; and Hilliard, Ohio*

ABSTRACT

Objective: Prosthetic grafts are often needed in open vascular procedures. However, the smaller diameter prosthetic grafts (<6 mm) have low patency and often result in complications from infection. Tissue-engineered vascular grafts (TEVGs) are a promising replacement for small diameter prosthetic grafts. TEVGs start as a biodegradable scaffold to promote autologous cell proliferation and functional neotissue regeneration. Owing to the limitations of graft materials; however, most TEVGs are rigid and easily kinked when implanted in limited spaces, which precludes clinical application. We have developed a novel corrugated nanofiber graft to prevent kinking.

Methods: TEVGs with corrugated walls (5-mm internal diameter by 10 cm length) were created by electrospinning a blend of poly-ε-caprolactone and poly(L-lactide-co-caprolactone). The biodegradable grafts were then implanted between the carotid artery and the external jugular vein in a U-shape using an ovine model. TEVGs were implanted on both the left and right side of a sheep (n = 4, grafts = 8). The grafts were explanted 1 month after implantation and inspected with mechanical and histologic analyses. Graft patency was confirmed by measuring graft diameter and blood flow velocity using ultrasound, which was performed on day 4 and every following week after implantation.

Results: All sheep survived postoperatively except for one sheep that died of acute heart failure 2 weeks after implantation. The graft patency rate was 87.5% (seven grafts out of eight) with one graft becoming occluded in the early phase after implantation. There was no significant kinking of the grafts. Overall, endothelial cells were observed in the grafts 1 month after the surgeries without graft rupture, calcification, or aneurysmal change.

Conclusions: Our novel corrugated nanofiber vascular graft displayed neotissue formation without kinking in large animal model. (JVS—Vascular Science 2020;1:100-8.)

Clinical Relevance: This basic science research article reported tissue-engineered vascular grafts for arteriovenous shunt procedures. Nanofibrous grafts were electrospun with polyglycolic acid and poly-ε-caprolactone with a corrugated wall design to prevent graft kinking. The tissue-engineered vascular grafts were then implanted in U-shape between the carotid artery and the external jugular vein of an ovine model. This graft had 87.5% patency rate and did not display significant kinking. Overall, re-endothelialization was observed in the grafts one month after the surgeries without graft rupture, calcification or aneurysmal change. This graft is a promising alternative to small diameter prosthetic grafts.

Keywords: Tissue-engineered vascular grafts; Smaller diameter prosthetic grafts; Large animal study; Corrugated nanofiber vascular graft; Arteriovenous shunt

In patients with end-stage renal disease (ESRD), vascular grafts are used to establish a direct arteriovenous (AV) shunt for hemodialysis (HD). Autogenous fistulas are preferred for access whenever possible, for example, from the brachiocephalic vein of the arm. However, patients with kidney failure often have scant vessels or suffer from stenotic arteries. Thus, autologous grafts are not readily available and, when accessible, the grafts are eventually exhausted after multiple HD procedures. Sometimes, the grafts are made of synthetic materials such as expanded polytetrafluoroethylene (PTFE) or Dacron. However, synthetic grafts are only implanted for middle to large diameter vessels. These synthetic grafts have been found inadequate to replace small diameter vessels for bypass or reconstruction operations. Specifically, intimal hyperplasia and thrombosis owing to foreign body reaction impede the use of these materials in grafts.[1,2] Synthetic materials are also susceptible to catheter-related blood stream infections in patients undergoing HD.[3] In general, the patency of the synthetic grafts remains low, with reported primary and secondary patency rates of PTFE at 1 year after the operation of 43%

From the Division of Cardiac Surgery, Johns Hopkins Hospital, Baltimore[a]; and the Nanofiber Solutions, LLC, Hilliard.[b]

The vascular grafts used in this study were provided by Nanofibersolutoins. NH received research funding and grafts for this study from Nanofibersolutions.

Correspondence: Narutoshi Hibino, MD, PhD, Division of Cardiac Surgery, Johns Hopkins Hospital Zayed 7107, 1800 Orleans St, Baltimore, MD 21287 (e-mail: nhibino1@jhmi.edu).

The editors and reviewers of this article have no relevant financial relationships to disclose per the JVS-Vascular Science policy that requires reviewers to decline review of any manuscript for which they may have a conflict of interest.

2666-3503

https://doi.org/10.1016/j.jvssci.2020.03.003

and 64%, respectively.[4] Overall, because of the sustained challenges with autologous and synthetic grafts sources, alternative vascular prostheses are sought to perform the AV shunt procedures for HD and cardiovascular operations.

Tissue-engineered vascular grafts (TEVGs) have been proposed as an alternative to address the challenges with current vascular prostheses.[5-10] TEVGs are a biodegradable graft template serving as a temporary scaffold that transforms into and regenerates vascular tissue. The materials that have been used for TEVGs include synthetic biodegradable polymers and blends with natural proteins such as collagen, elastin, gelatin, and albumin.[5-10] TEVGs are mainly used as venous conduits and are exposed to lower pressures than in AV shunts, even though AV shunts are not under high pressure unless there is outflow stenosis.[6,11] Wystrychowski et al[12] have reported implantation of TEVGs in high pressure circulation for HD access. Several other clinical trials also assessed TEVGs under pressures suitable for AV shunts.[13,14] In all cases, these TEVGs were seeded with cells before implantation, which is a costly additional step that increases the risks of infection.[15] Additionally, the TEVGs were implanted as a straight conduit, which is not akin to AV shunt procedures in patients wherein the graft needs to be implanted at an angle to have adequate puncture sites for HD.[16] These TEVGs are at risk of kinking if bent, for example, into a U-shape.[17] The addition of corrugations throughout the graft structure has been suggested as a strategy to decrease the risk of kinking.[18] In addition, the grafts made from a blend of the biodegradable polymers poly(L-lactide-co-caprolactone) (PLCL) and polyglycolic acid (PGA) dilated and degraded quickly.[16]

In this study, we used a poly-ε-caprolactone (PCL)/PLCL polymer blend and developed TEVGs with corrugations that were implanted with a U-shape in a sheep model. We then assessed the performance. PCL degraded at a slower rate than the previously used PGA.[16,19] Thus, the inclusion of PCL in the blend with PLCL is hypothesized to slow the graft degradation rate such that the prosthesis can withstand the high-pressure arterial system. The corrugations of the TEVGs were made during graft fabrication by electrospinning. Using an anatomically accurate mandrel during this process can be used to further develop patient-matched scaffolds.[16] The previously established bilateral AV shunt procedure for the large animal model had to be adapted to accommodate implantation with the new graft configuration. The grafts were then implanted into the cervical region of the sheep and tested for biocompatibility. This step was followed by validation of biomechanical properties, and proliferation of endothelial and smooth muscle progenitor cells. Taken together, these assessments and changes to graft morphology, material, and implant configuration serve toward understanding the applicability of TEVGs as small diameter vascular prostheses.

ARTICLE HIGHLIGHTS

- **Type of Research:** Single-center, prospectively collected data
- **Key Findings:** Tissue-engineered vascular grafts implanted between the carotid artery and the external jugular vein in a sheep model (n = 4, grafts = 8) had an average patency rate of 87.5%, and re-endothelialization was observed 1 month after surgery without graft rupture, calcification, or aneurysmal change.
- **Take Home Message:** Our novel corrugated nanofiber vascular graft, developed by electrospinning a blend of poly-ε-caprolactone and poly(L-lactide-co-caprolactone), displayed neotissue formation without kinking in a large animal model. It is a promising alternative for vascular surgery procedures requiring a small diameter prosthetic graft, and the achieved results warrant further research.

METHODS

Scaffold fabrication. PCL/PLCL scaffolds are created by co-electrospinning method as previously described[20] with a customized graft length of 10 cm and inner diameter of 5 mm. Initially, 6 wt% PCL and 5 wt% PCL were dissolved in hexafluoroisopropanol and stirred with a magnetic stir bar for at least 24 hours at room temperature. In separate syringes, the PLCL solution was dispensed at a flow rate of 5.0 mL/h, whereas the PCL solution was dispensed at a flow rate of 4.2 mL/h to create a graft scaffold with a PCL:PLCL weight ratio of 1:1. Both solutions were simultaneously electrospun onto a grounded mandrel that was positioned 20 cm from needle tip and rotated at 100 revolutions per minute, with a +25-kV charge applied. After electrospinning, nanofibers were deposited onto the ground mandrel until the desired wall thickness was achieved. The electrospun scaffold was then removed from the mandrel, and the wall thickness was measured with a laser micrometer (Keyence, Osaka, Japan). The scaffolds were then corrugated by wrapping a 260-μm diameter monofilament around the scaffold at a specified threads per inch count and specified thread tension. The scaffold was then longitudinally compressed to 30% to 45% of its original length and allowed to set for 24 hours. It was then elongated to 50% to 65% of its original length and the monofilament was removed. The scaffolds were sectioned into 10-cm lengths, plasma treated, packaged in Tyvek pouches, and terminally sterilized with gamma irradiation.

Mechanical testing. Compliance and burst pressure data were acquired with the samples immersed in PBS using a universal mechanical testing machine (MTS System Corporation, Minn) as previously described.[20] Put briefly, data were acquired using a load frame fitted with a 50-pound load cell with a force resolution of 10^{-4} pounds and a linear displacement resolution of 10^{-8} inches. Compliance testing was performed using a displacement velocity of 1.5 mm per minute and an acquisition rate of 4 data points per second using Laplace's law[20] to correlate linear force and displacement to compliance. Burst pressure testing was performed using a displacement velocity of 50 mm/min and an acquisition rate of 4 data points per second using Laplace's law[20] to correlate linear force and displacement to burst pressure. Samples were placed around two parallel L-shaped steel rods; one rod was attached to the base of the universal testing machine and the other to the load cell. The samples were strained perpendicularly to the length of the samples. Compliance was calculated using systolic and diastolic pressure of 120 mm Hg and 80 mm Hg, respectively. The burst pressure was calculated as the maximum force immediately before failure. Kink testing was completed the same way as described in ISO 7198 (2016) A.5.8 — Kink diameter/Radius. Briefly, a cylindrical mandrel is used to determine the kink radius. This test is accomplished by forming a loop with the test sample and pulling the ends of the sample in opposite directions to decrease the loop until a kink is observed. The appropriately sized cylindrical mandrel is placed within the loop to measure the kink diameter and that mandrel size is recorded.

Graft implantation. The Animal Care and Use Committee at Q-Test Laboratories (Columbus, Ohio) approved the care, use, and monitoring of animals for sheep experiments. Four custom-made nanofiber TEVGs were implanted bilaterally as AV shunts between the common carotid artery (CCA) to the ipsilateral external jugular vein (EJV) in four sheep. Implantation was accomplished as previously described.[16] Briefly, all sheep were anesthetized with 1% to 2% isoflurane and positioned in the dorsal recumbency during surgery. Heparin (100 IU/kg) was administrated intravenously after exposure of the bilateral CCA and EJV. Standard vascular anastomosis was performed with a 7-0 Prolene suture (Ethicon Inc, Somerville, NJ). Hemostasis was obtained, and the muscle, subcutaneous tissue, and dermal incision layers were closed. Antibiotic treatment (cefazolin) was administrated intraoperatively and for 7 days postoperative. All sheep were maintained on a daily oral medication of aspirin (325 mg/d) until the end of the study. Serial color Doppler ultrasound examinations were performed to estimate graft patency and to measure the lumen diameter and the blood flow velocity. Animals were humanely killed by pentobarbital sodium one month after implantation.

Ultrasound examination. Color Doppler ultrasound was performed every week after implantation to determine graft patency, the lumen diameter of TEVG, the wall thickness of TEVG, and the blood flow velocity of TEVG. Both the anastomosis site and the middle of grafts were measured. If blood flow was observed at all of the sites, the graft was determined to be patent. Ultrasound images were assembled by using a Philips HD11 XE ultrasound machine (Philips, Amsterdam, the Netherlands) and a probe of adequate frequency (Philips L15-7io) to assess the vascular structures.

Histology and immunohistochemistry. The middle parts of explanted TEVG samples were fixed in 10% formalin for 24 hours at 4°C, and then embedded in paraffin for standard histologic analysis with hematoxylin and eosin, Masson's trichrome, Verhoeff-Van Gieson (VVG), and von Kossa (VK) staining. For VK staining, human placenta tissue was used as a positive control. For immunohistochemistry, the tissue sections were deparaffinized, rehydrated, and blocked for endogenous peroxidase activity and nonspecific staining. The primary antibodies used included von Willebrand Factor (1:2000; Dako, Glostrup, Denmark), α-smooth muscle actin (1:500; Dako), and CD68 (1:200; Abcam, Cambridge, UK). Biotinylated secondary antibodies and streptavidinated horseradish peroxidase were then used before the color development of chromogenic reaction with 3,3-diaminobenzidine (Vector Laboratories, Burlingame, Calif). Nuclei counterstaining was performed with Gill's hematoxylin (Vector Laboratories).

Histologic and quantitative analyses. The remaining scaffold area was measured by using polarized light and analyzed with Image J software (Image Processing and Analysis in Java; National Institutes of Health, Bethesda, Md). The macrophages that were identified by positive CD68 expression were quantified for each explanted scaffold. Four sections of each individual sample were counted at 40 × (high powered field) and then averaged.

Statistical analysis. For all experiments, data are represented as mean ± standard deviation. Ultrasound data (lumen diameter and wall thickness) and diameter measured with macrograph and mechanical property (burst pressure and compliance) were analyzed via one-way analysis of variance with Tukey's multiple-comparisons test. A *t*-test was performed and a *P* value of less than .01 was considered statistically significant.

RESULTS

Graft morphology. In comparison with a commercial vascular prosthesis (Fig 1, *A*), the TEVG graft (Fig 1, *B*) could be bent 180° without kinking because of its corrugated anatomy (Fig 1, *C*). This property was

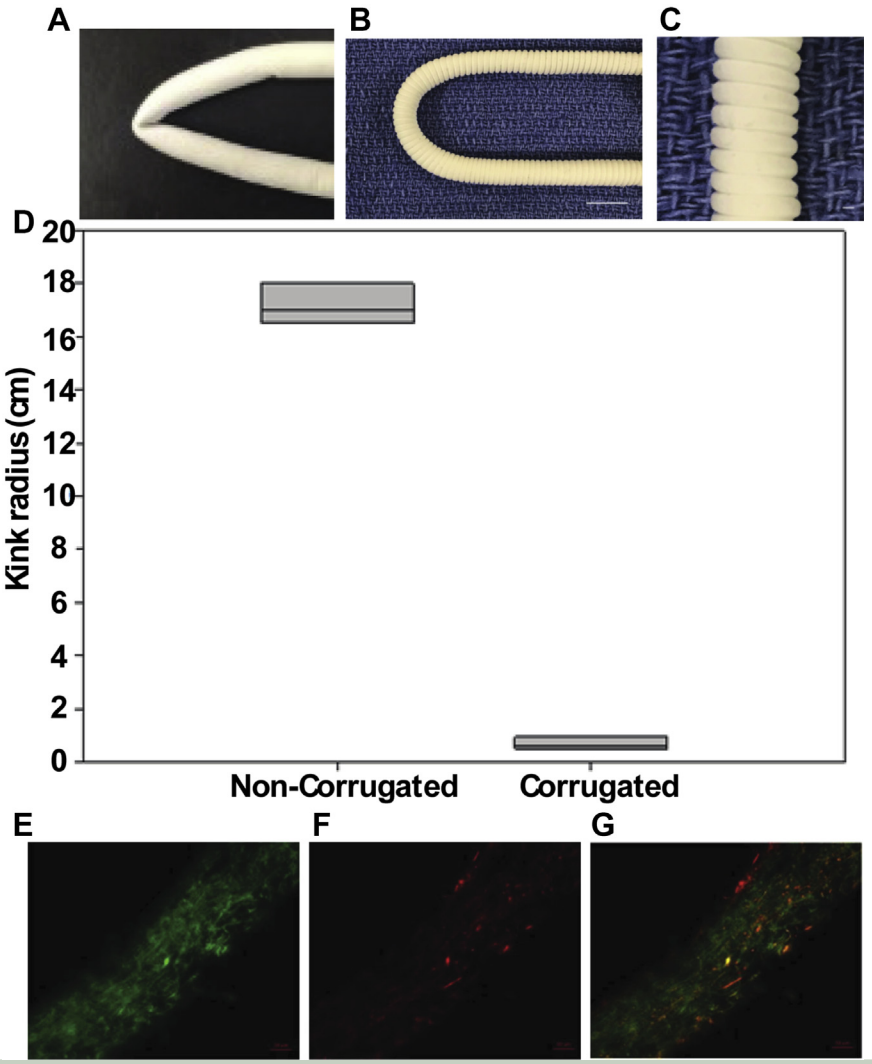

Fig 1. A, Image of EXXCEL SOFT vascular graft (Maquet Cardiovascular, Wayne, NJ) that exhibits kinking upon a 180° bend. **B,** The TEVG graft that has corrugations to maintain flexibility and conformability upon a 180° bend. Scale bar = 10 mm. **C,** Close-up of the TEVG graft corrugations. Scale bar = 1 mm. **D,** A comparison of the kink radius for the noncorrugated and corrugated grafts. **E-G,** Demonstration of electrospinning with a different dye used in each polymer. Scale bar = 50 μm.

demonstrated by measuring the kink radius for both noncorrugated and corrugated TEVGs made from the PLCL-PGA blend (Fig 1, *D*). The noncorrugated TEVG had a kink radius that was approximately 16 times larger than the corrugated graft. Fluorescent imaging highlighted the different polymer components of the graft with one stained with fluorescein isothiocyanate dye (Fig 1, *E*) and the other with the rhodamine dye (Fig 1, *F*). This morphologic assessment established that the graft is a blend of both these components (Fig 1, *G*).

Serial ultrasound examinations. One sheep died owing to acute heart failure 2 weeks after surgery. Ultrasound analysis showed that one out of the eight implanted grafts was occluded 1 week after implantation. The lumen diameter and the wall thickness of the TEVGs did not statistically significantly increase throughout the 4-week period (Fig 2, *A, B*). The blood flow velocity did not change significantly and the blood flow by velocity-time integrals slightly increased (Fig 2, *C, D*).

Graft assessment upon explantation. There was no thrombus on gross examination of the grafts, aneurysmal formation or rupture (Fig 3, *A*). Furthermore, the arterial (Fig 3, *B*) and venous (Fig 3, *C*) anastomosis sites of TEGVs displayed no apparent stenosis or thrombus. The intraoperative picture is shown in Fig 3, *D*, and represented as a schematic in Fig 3, *E*. Overall, the inner diameters, measured macroscopically, at both anastomosis site and the middle of graft ranged from

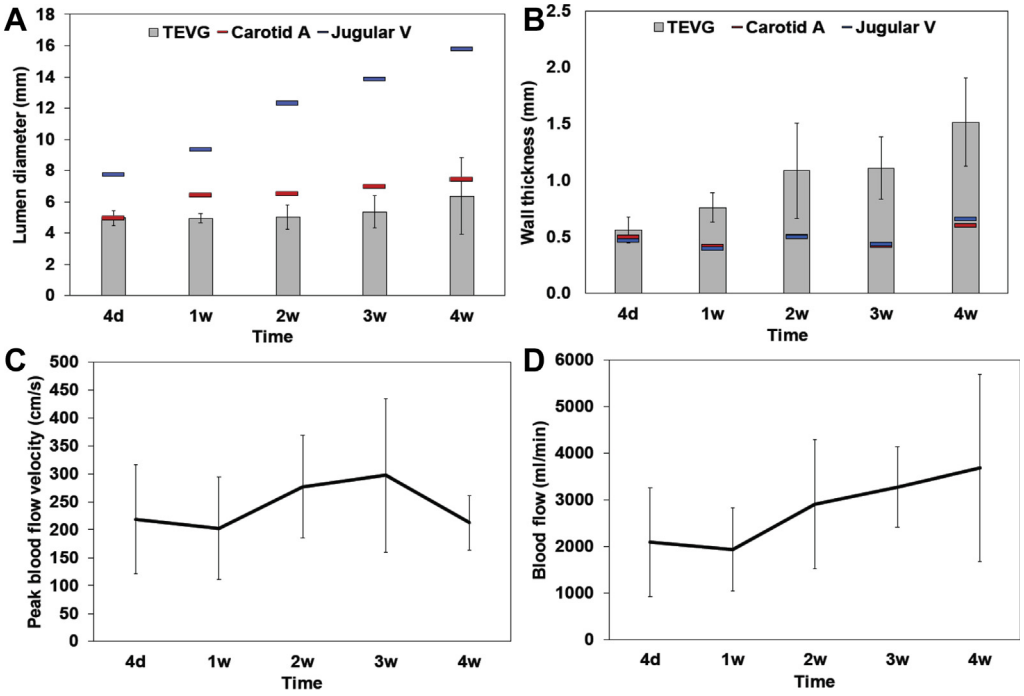

Fig 2. Serial ultrasound parameters of the tissue-engineered vascular graft (*TEVG*) at 4 days, 1 week, 2 weeks, 3 weeks, and 4 weeks after the surgery. **(A)** Lumen diameter and **(B)** wall thickness of TEVG. **(C)** Peak blood flow velocity measured by velocity-time integrals and **(D)** blood flow analysis.

approximately 5 to approximately 6.5 mm (Fig 3, *F*). The primary patency was 100% for about 4 days and 87.5% for the 28 days.

Mechanical properties of the TEVG. The burst pressure of implanted TEVGs (2126 ± 1027 mm Hg) was significantly lower than the preoperative TEVGs (11,997 ± 2236 mm Hg), the carotid artery (8155 ± 780 mm Hg), and the jugular vein (9119 ± 1403 mm Hg) (Fig 4, *A*). Compliance of the TEVGs (5.1 ± 1.6% mm Hg) was significantly lower than the carotid artery (13.7 ± 2.5% mm Hg) and the jugular vein (8.1 ± 2.7% mm Hg) (Fig 4, *B*). However, the compliance of implanted TEVGs is not significantly different from the preoperative TEVGs (4.8 ± 0.2% mm Hg) (Fig 4, *B*).

Histologic analysis of the TEVG. Hematoxylin and eosin staining revealed extensive cellular infiltration in the TEVGs. Therefore, the scaffold parameters, such as pore size and fiber diameter, allowed host cell infiltration. In addition, the VVG staining demonstrated that the elastin composition of the TEVG was comparable to that of native CCA (Fig 5, *I* and *K*). The VK staining (Fig 5, *N*) showed no evidence of ectopic calcification. On the luminal surface of the grafts, a cellular monolayer was positively stained with von Willebrand factor, which is an indication of presence of endothelial cells. This was also the case for the native vessels (Fig 5, *R* and *S*). Smooth muscle cells (SMCs) are one of the imperative constituents for vascular function.[21,22] Mature contractile vascular SMCs were identified using α-smooth muscle actin antibody. A multilayered population of α-smooth muscle actin–positive cells was present under the endothelial layer. CD68-positive macrophages are the main cell population in the inflammation-mediated process of vascular remodeling in biodegradable scaffolds.[23,24] Substantial CD68-positive macrophages were detected in our TEGVs (Fig 6, *C*).

Scaffold biodegradation. The remaining graft scaffold was quantified by polarized microscopy (Fig 6, *D*). Although the scaffold did not completely degrade over the follow-up term, the positive area of polarized light after 1 month was 16.10 ± 1.39%. The TEVG scaffold remained mainly in the external side.

DISCUSSION

Demands for TEVGs that promote small diameter vessel regrowth with a high patency rate, durability and resistance to infection are increasing with cardiovascular disease and ESRD.[14,25,26] In this study, we assessed cell-free PCL/PLCL electrospun scaffolds to develop TEVGs for bilateral AV shunts in the neck region of a sheep model. The procedure was expanded here to accommodate the implantation of grafts in a configuration that mimics those in HD procedures, in which the graft is implanted with a U-shape. It has also been suggested that using a pleated morphology decreases the risk of graft kinking.[18]

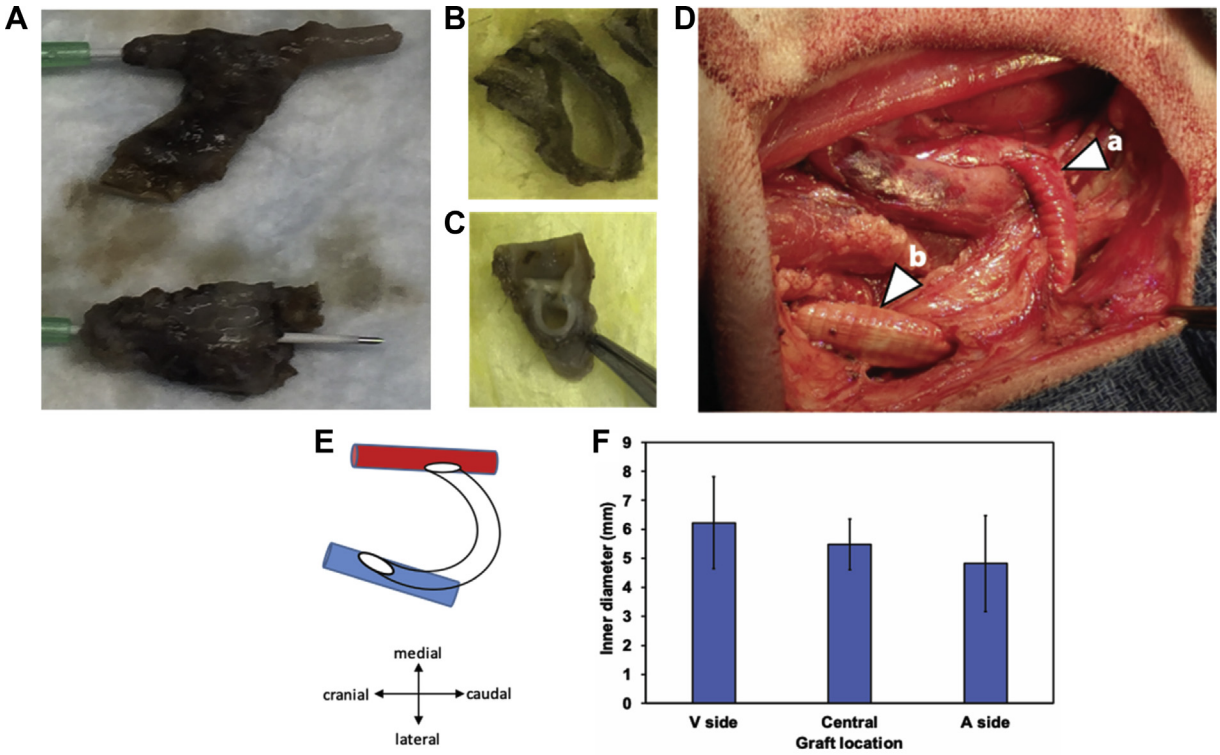

Fig 3. A, Macrograph of the tissue-engineered vascular graft (*TEVG*), the carotid artery, and the jugular vein. Cross-sectional images of anastomosis site with **(B)** the jugular vein and **(C)** the carotid artery. **D,** Image of the surgical implantation with arrows indicating (*a*) the arterial side and (*b*) the venous side of anastomosis sites. **E,** Schema of TEVG implantation surgery. **F,** Largest inner diameters measured with the unaided eye. No significant difference was observed across the graft arterial anastomosis site and venous site.

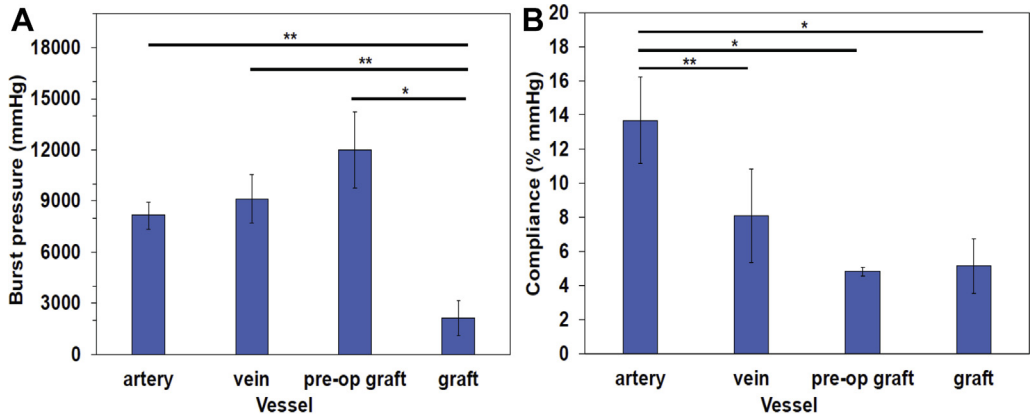

Fig 4. Mechanical property of the tissue-engineered vascular graft (*TEVG*). **(A)** Burst pressure and **(B)** compliance. Asterisk indicates statistical significance between the two groups. *$P < .001$; **$P < .01$.

TEVGs in this study were made with corrugations, which is a novel approach in biodegradable graft design. When we create a U-shape with a PTFE graft, this graft showed kinks (Fig 1, *A*). Therefore, the PTFE graft was not used as a control because this kinking leads to occlusion. Given the kink radius data (Fig 1, *D*), the same TEVG without corrugation likewise could not serve as a control owing to kinking. The primary patency during this term was 87.5%, which is promising and exceeds the patency of grafts implanted in a swine model for same duration in a different study.[17] The latter study used grafts made from the small intestinal submucosa and still outperformed commercial Gortex controls.[17] The burst pressure of the TEVG (2126 ± 1027 mm Hg) was high enough for the graft to withstand normal blood pressure and was close to that of human saphenous vein (1673 ±

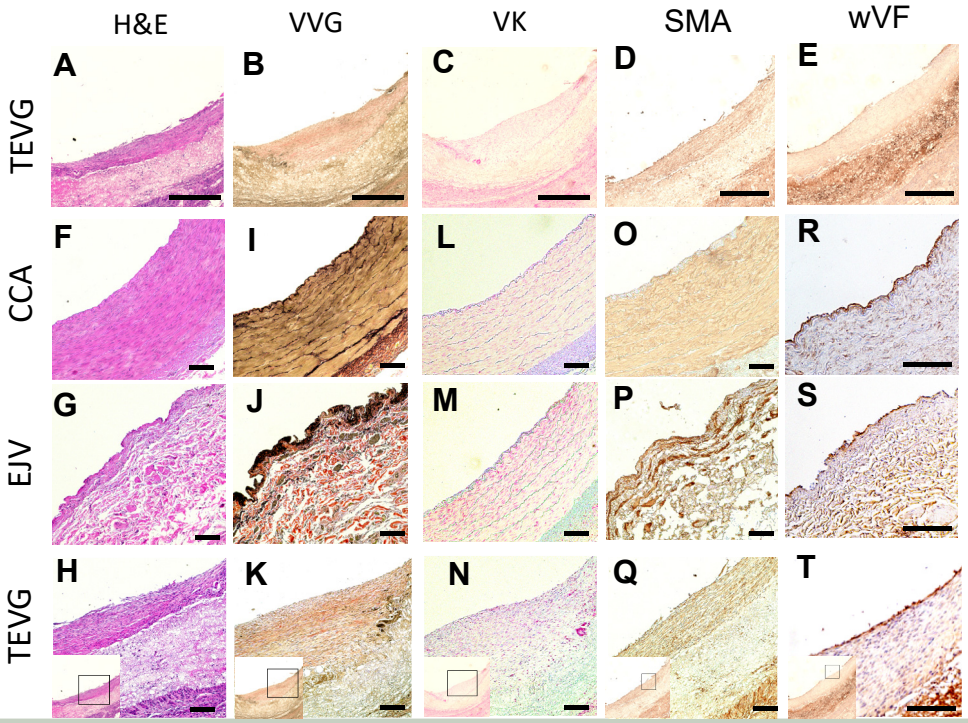

Fig 5. Immunohistochemistry of vascular grafts, carotid artery and jugular vein 4 weeks after surgery. H&E **(A** and **F-H)**, VVG **(B** and **I-K)**, VK staining **(C** and **L-N)**, SMA immunostaining **(D** and **O-Q)** and vWF immunostaining **(E** and **R-T)**. Magnification is ×4 **(A-E).** Magnification is ×10 **(F-Q)**. Magnification is ×20 **(R-T)**. Scale bar is 750 μm for ×4 magnification, 350 μm for ×10 magnification, and 150 μm for ×20 magnification. *CCA*, Common carotid artery; *EJV*, external jugular vein; *H&E*, hematoxylin and eosin; *SMA*, α-smooth muscle actin antibody; *TEVG*, tissue-engineered vascular graft; *VK*, von Kossa; *VVG*, Verhoeff-Van Gieson; *vWF*, von Willebrand factor.

306 mm Hg).[27] However, the decrease in burst pressure and increase in graft diameter may be the beginning of a trend toward expansion as the lumen diameter of the graft increased 20% between weeks 3 and 4, and wall thickness tended to increase in ultrasound examination. Our sample size was small, and the follow-up term was only 4 weeks, meaning long-term follow-up with an appropriate sample size is essential.

The remaining scaffold area 1 month after implantation was 16.1 ± 1.39%. The degradation rate of our previous study[5] for a small animal (rat) model was faster, with 9.1 ± 5.4% remaining 6 months after implantation. The latter was made from a different PCL/Chitosan polymer blend.[5] Our TEVG scaffolds may be preferable because longer degradation rates could lead to poor neotissue formation and hamper vascularization of the graft wall.[28,29] Overall, further work is needed to evaluate the optimal degradation rate and to determine the mechanical integrity of the TEVG scaffolds so as to avoid surgical complications such as stenosis or occlusion owing to a low degradation rate or dilatation or aneurysmal formation owing to a high degradation rate. Histologically, the luminal surface of the TEVG had a confluent layer of endothelial cells stained positively with the von Willebrand factor. Although this factor is not specific to endothelial cells, there is no specific marker for endothelial cells in sheep, and so the von Willebrand factor has been used in many studies as a sufficient alternative.[5,16,30-35] We need further functional testing for typical cellular functions of the endothelial layer, such as secretion of tissue plasminogen activator, to assess whether there has been true endothelialization of the graft.

In this ovine model, we could observe feasible endothelial cells of TEVG, but it is not certain if this will occur in humans to the same extent. The TEVGs had contractile vascular SMCs. Extracellular matrix deposition was represented by Masson's trichrome staining and moderate elastin composition was assessed through VVG staining. The TEVG histologic analysis paralleled the native CCA, suggesting that the biodegradable grafts underwent vascular remodeling. SMCs also play a vital role in maintaining and remodeling the extracellular matrix of blood vessels.[36] Still, excessive SMC proliferation may lead to intimal hyperplasia, eventually resulting in vascular stenosis or complete occlusion.[37] Our 1-month follow-up study is insufficient to confirm if the vascular SMCs in

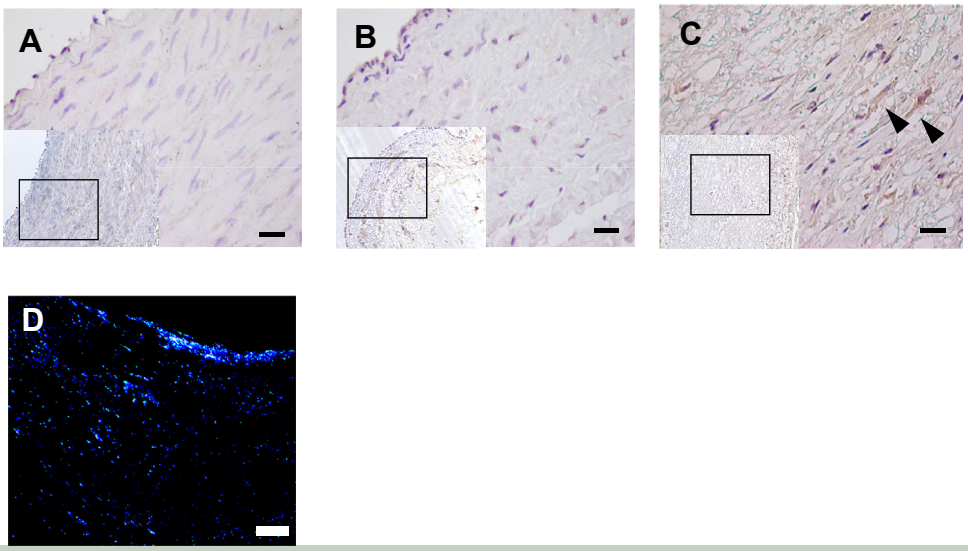

Fig 6. Histologic findings of CD68-positive macrophage. **(A)** Common carotid artery (CCA), **(B)** external jugular vein (EJV), and **(C)** tissue-engineered vascular graft (TEVG) are ×20. Scale bar is 20 μm. **D,** Polarized light microscopy of the remaining TEVG graft scaffold. Scale bar: 100 μm.

the TEVG serve the same function as SMCs in native vessels or would eventually lead to occlusive stenosis.[38-40] Thus, future studies should focus on longer term assessments of the TEVGs. Last, the CCA-EJV shunt in sheep is subject to a larger blood flow than the AV shunts in patients with ESRD. Thus, prospective translational efforts to human clinical trials should consider the differences and limitations of this study, particularly with respect to the site of implantation.

CONCLUSIONS

A biodegradable PCL/PLCL polymer blend was used to electrospin corrugated TEVGs that were then assessed under high pressure and while bent in the AV shunt of a large animal model. TEVGs with corrugations demonstrated kink resistance and endothelialization and neotissue formation. This novel design of a cell-free nanofiber graft has great potential for future applications as the AV shunt graft for the management of patients with ESRD.

We thank Sayali Dharmadhikari from Nationwide Children's Hospital.

AUTHOR CONTRIBUTIONS

Conception and design: HM, TI, SA, EY, CO, CL, IP, KN, JJ
Analysis and interpretation: HM, TI, SA, EY, CO, CL, IP, KN, JJ
Data collection: HM, TI, SA, EY, CO, CL, IP, KN, JJ
Writing the article: HM, TI, SA, EY, CO, CL, IP, KN, JJ
Critical revision of the article: HM, TI, SA, EY, CO, CL, IP, KN, JJ
Final approval of the article: HM, TI, SA, EY, CO, CL, IP, KN, JJ
Statistical analysis: Not applicable
Obtained funding: Not applicable
Overall responsibility: HM

REFERENCES

1. Pashneh-Tala S, MacNeil S, Claeyssens F. The tissue-engineered vascular graft-past, present, and future. Tissue Eng Part B Rev 2015;22:68-100.
2. Zilla P, Bezuidenhout D, Human P. Prosthetic vascular grafts: wrong models, wrong questions and no healing. Biomaterials 2007;28:5009-27.
3. Labriola L, Pochet J-M. Any use for alternative lock solutions in the prevention of catheter-related blood stream infections? J Vasc Access 2017;18(1 Suppl):S34-8.
4. Cinat ME, Hopkins J, Wilson SE. A prospective evaluation of PTFE graft patency and surveillance techniques in hemodialysis access. Ann Vasc Surg 1999;13:191-8.
5. Fukunishi T, Best CA, Sugiura T, Shoji T, Yi T, Udelsman B, et al. Tissue-engineered small diameter arterial vascular grafts from cell-free nanofiber PCL/Chitosan scaffolds in a sheep model. PLoS One 2016;11:e0158555.
6. Hibino N, McGillicuddy E, Matsumura G, Ichihara Y, Naito Y, Breuer C, et al. Late-term results of tissue-engineered vascular grafts in humans. J Thorac Cardiovasc Surg 2010;139:431-6.e2.
7. Tamimi E, Ardila DC, Haskett DG, Doetschman T, Slepian MJ, Kellar RS, et al. Biomechanical comparison of glutaraldehyde-crosslinked gelatin fibrinogen electrospun scaffolds to porcine coronary arteries. J Biomech Eng 2016;138:0110011-2.
8. Tillman BW, Yazdani SK, Lee SJ, Geary RL, Atala A, Yoo JJ. The in vivo stability of electrospun polycaprolactone-collagen scaffolds in vascular reconstruction. Biomaterials 2009;30:583-8.
9. Wise SG, Byrom MJ, Waterhouse A, Bannon PG, Ng MKC, Weiss AS. A multilayered synthetic human elastin/

polycaprolactone hybrid vascular graft with tailored mechanical properties. Acta Biomaterialia 2011;7:295-303.
10. Zhang M, Wang K, Wang Z, Xing B, Zhao Q, Kong D. Small-diameter tissue engineered vascular graft made of electrospun PCL/lecithin blend. J Mater Sci Mater Med 2012;23:2639-48.
11. Sugiura T, Matsumura G, Miyamoto S, Miyachi H, Breuer CK, Shinoka T. Tissue-engineered vascular grafts in children with congenital heart disease: intermediate term follow-up. Semin Thorac Cardiovasc Surg 2018;30:175-9.
12. Wystrychowski W, Cierpka L, Zagalski K, Garrido S, Dusserre N, Radochonski S, et al. Case study: first implantation of a frozen, devitalized tissue-engineered vascular graft for urgent hemodialysis access. J Vasc Access 2011;12:67-70.
13. Lawson JH, Glickman MH, Ilzecki M, Jakimowicz T, Jaroszynski A, Peden EK, et al. Bioengineered human acellular vessels for dialysis access in patients with end-stage renal disease: two phase 2 single-arm trials. Lancet 2016;387:2026-34.
14. Wystrychowski W, McAllister TN, Zagalski K, Dusserre N, Cierpka L, L'Heureux N. First human use of an allogeneic tissue-engineered vascular graft for hemodialysis access. J Vasc Surg 2014;60:1353-7.
15. Zhou M, Qiao W, Liu Z, Shang T, Qiao T, Mao C, et al. Development and in vivo evaluation of small-diameter vascular grafts engineered by outgrowth endothelial cells and electrospun chitosan/poly(ε-caprolactone) nanofibrous scaffolds. Tissue Eng A 2014;20:79-91.
16. Siang OC, Takuma F, Han LR, Kevin N, Huaitao Z, Elizabeth W, et al. Bilateral Arteriovenous shunts as a method for evaluating tissue-engineered vascular grafts in large animal models. Tissue Eng Part C Methods 2017;23:728-35.
17. Valencia Rivero KT, Jaramillo Escobar J, Galvis Forero SD, Miranda Saldaña MC, López Panqueva RDP, Sandoval Reyes NF, et al. New regenerative vascular grafts for hemodialysis access: evaluation of a preclinical animal model. J Invest Surg 2018;31:192-200.
18. Bode M, Mueller M, Zernetsch H, Glasmacher B. Electrospun vascular grafts with anti-kinking properties. Current Directions in Biomedical Engineering 2015;524.
19. Pan Y, Zhou X, Wei Y, Zhang Q, Wang T, Zhu M, et al. Small-diameter hybrid vascular grafts composed of polycaprolactone and polydioxanone fibers. Sci Rep 2017;7:3615.
20. Johnson J, Ohst D, Groehl T, Hetterscheidt S, Jones M. Development of novel, bioresorbable, small-diameter electrospun vascular grafts. J Tissue Sci Eng 2015;6.
21. Bochaton-Piallat M-L, Bäck M. Novel concepts for the role of smooth muscle cells in vascular disease: towards a new smooth muscle cell classification. Cardiovasc Res 2018;114:477-80.
22. Michel J-B, Li Z, Lacolley P. Smooth muscle cells and vascular diseases. Cardiovasc Res 2012;95:135-7.
23. Lash GE, Pitman H, Morgan HL, Innes BA, Agwu CN, Bulmer JN. Decidual macrophages: key regulators of vascular remodeling in human pregnancy. J Leukocyte Biol 2016;100:315-25.
24. Pullamsetti SS, Savai R. Macrophage regulation during vascular remodeling: implications for pulmonary hypertension therapy. Am J Respir Cell Mol Biol 2017;56:556-8.
25. Benjamin EJ, Virani SS, Callaway CW, Chamberlain AM, Chang AR, Cheng S, et al. Heart disease and stroke statistics - 2018 update: a report from the American Heart Association. Circulation 2018;137:e67-492.
26. McAllister TN, Maruszewski M, Garrido SA, Wystrychowski W, Dusserre N, Marini A, et al. Effectiveness of haemodialysis access with an autologous tissue-engineered vascular graft: a multicentre cohort study. Lancet 2009;373:1440-6.
27. L'Heureux N, Dusserre N, Konig G, Victor B, Keire P, Wight TN, et al. Human tissue-engineered blood vessels for adult arterial revascularization. Nat Med 2006;12:361-5.
28. de Valence S, Tille J-C, Mugnai D, Mrowczynski W, Gurny R, Möller M, et al. Long term performance of polycaprolactone vascular grafts in a rat abdominal aorta replacement model. Biomaterials 2012;33:38-47.
29. Tara S, Kurobe H, Rocco KA, Maxfield MW, Best CA, Yi T, et al. Well-organized neointima of large-pore poly(L-lactic acid) vascular graft coated with poly(L-lactic-co-ε-caprolactone) prevents calcific deposition compared to small-pore electrospun poly(L-lactic acid) graft in a mouse aortic implantation model. Atherosclerosis 2014;237:684-91.
30. Hoerstrup SP, Cummings Mrcs I, Lachat M, Schoen FJ, Jenni R, Leschka S, et al. Functional growth in tissue-engineered living, vascular grafts: follow-up at 100 weeks in a large animal model. Circulation 2006;114(1 Suppl):I159-66.
31. Brennan MP, Dardik A, Hibino N, Roh JD, Nelson GN, Papademitris X, et al. Tissue-engineered vascular grafts demonstrate evidence of growth and development when implanted in a juvenile animal model. Ann Surg 2008;248:370-7.
32. Syedain ZH, Meier LA, Lahti MT, Johnson SL, Tranquillo RT. Implantation of completely biological engineered grafts following decellularization into the sheep femoral artery. Tissue Eng Part A 2014;20:1726-34.
33. Fukunishi T, Best CA, Sugiura T, Opfermann J, Ong CS, Shinoka T, et al. Preclinical study of patient-specific cell-free nanofiber tissue-engineered vascular grafts using 3-dimensional printing in a sheep model. J Thorac Cardiovasc Surg 2017;153:924-32.
34. Pepper VK, Clark ES, Best CA, Onwuka EA, Sugiura T, Heuer ED, et al. Intravascular ultrasound characterization of a tissue-engineered vascular graft in an ovine model. J Cardiovasc Transl Res 2017;10:128-38.
35. Dahan N, Sarig U, Bronshtein T, Baruch L, Karram T, Hoffman A, et al. Dynamic autologous reendothelialization of small-caliber arterial extracellular matrix: a preclinical large animal study. Tissue Eng Part A 2017;23:69-79.
36. Ponticos M, Smith BD. Extracellular matrix synthesis in vascular disease: hypertension, and atherosclerosis. J Biomed Res 2014;28:25-39.
37. Rodriguez VM, Grove J, Yelich S, Pearson D, Stein M, Pevec WC. Effects of brachytherapy on intimal hyperplasia in arteriovenous fistulas in a porcine model. J Vasc Interv Radiol 2002;13:1239-46.
38. Fogelstrand P, Mellander S, Mattsson E. Increased vascular injury reduces the degree of intimal hyperplasia following angioplasty in rabbits. J Vasc Res 2011;48:307-15.
39. Ikesue M, Matsui Y, Ohta D, Danzaki K, Ito K, Kanayama M, et al. Syndecan-4 deficiency limits neointimal formation after vascular injury by regulating vascular smooth muscle cell proliferation and vascular progenitor cell mobilization. Arterioscler Thrombos Vasc Biol 2011;31:1066-74.
40. Sata M, Saiura A, Kunisato A, Tojo A, Okada S, Tokuhisa T, et al. Hematopoietic stem cells differentiate into vascular cells that participate in the pathogenesis of atherosclerosis. Nat Med 2002;8:403.

Submitted Oct 8, 2019; accepted Mar 25, 2020.